Observation of Plasma Flow at the Magnetic Island in the Large Helical Device

K. Ida, N. Ohyabu, T. Morisaki, Y. Nagayama, S. Inagaki, K. Itoh, Y. Liang, K. Narihara, A. Yu. Kostrioukov, B. J. Peterson, K. Tanaka, T. Tokuzawa, K. Kawahata, H. Suzuki, A. Komori, and LHD Experimental Group

National Institute for Fusion Sciences, Toki, Gifu 509-5292, Japan

(Received 16 July 2001; published 20 December 2001)

Radial profiles of ion temperature and plasma flow are measured at the $n/m = 1/1$ magnetic island produced by external perturbation coils in the Large Helical Device. The sheared poloidal flows and sheared radial electric field are observed at the boundaries of the magnetic island, because the poloidal flow vanishes inside the static magnetic island. When the width of the magnetic island becomes large, the flow along the magnetic flux surface inside the magnetic island appears around the O point in the direction which reduces the shear of the poloidal flow at the boundary of the magnetic island.

DOI: 10.1103/PhysRevLett.88.015002 PACS numbers: 52.55.Hc, 52.50.Gj

The structure of magnetic islands is observed in various plasma experiments. The electron temperature profiles measured with Thomson scattering or electron cyclotron emission (ECE) signals shows a flattening inside the magnetic island [1]. On the other hand, density profile peaking inside the magnetic island is observed in JET and TEXTOR [2–4]. The density peaking is more significant when particles are fueled into the magnetic island by a pellet [2,3], which is observed in a soft x-ray signal as "snake" modulation in JET. These observations suggest that the particle diffusivity is low and there should be a pinch velocity towards the center of the island, which causes density peaking inside the magnetic island. These experimental observations suggest that the plasma space potential may have some structure inside the magnetic island. Recently the physics of magnetic islands was recognized to be important, after the observation of the significant effect of neoclassical tearing modes on the plasma confinement [5]. The recent observations of the internal transport barriers at or near the rational magnetic surface in tokamak plasmas imply the importance of magnetic islands in the plasma confinement [6]. This is because the drag due to the magnetic island produces the sheared flow and sheared radial electric field at the boundary of the magnetic island. A theoretical prediction has been made that the topological change of magnetic surfaces across the island can cause a transport barrier at the island [7]. The possible role of the island on the local variation of thermal diffusivity has been reported by RTP experiments [8]. However, no experimental results on the profiles of ion temperature and poloidal flow at the magnetic island have been reported, except for the probe measurements in TJ-II [9]. Although the structures of the radial electric field and the radial electric field shear are crucial parameters to understand the good confinement (low diffusivity) inside the magnetic island, there have been no clear measurements of poloidal flow or radial electric field inside the magnetic island. In this paper the clear observation of sheared poloidal flow (v_θ) and the resulting radial electric field (E_r) at the magnetic island are presented.

The Large Helical Device (LHD) is a toroidal helical magnetic device (Heliotron Device) with a major radius of $R_{ax} = 3.5$–4.1 m, an average minor radius of 0.6 m, and magnetic field 0.5–3 T [10,11]. It has $n/m = 1/1$ external perturbation coils, and the size of the magnetic island can be controlled up to 10 cm by changing the current of the perturbation coils, $I_{n/m=1/1}$. The radial profiles of E_r are derived from v_θ measured with charge exchange spectroscopy (CXS) at the midplane in LHD by using a charge exchange reaction between fully ionized neon impurity and atomic hydrogen from the neutral beam [12].

The direction of elongation of the plasma cross section in a plane through the major axis in LHD depends on the toroidal angle, ϕ, with the periodicity of ten (every 36°). Therefore the major radius for the location of the magnetic island depends on ϕ, even when the magnetic island is located at the constant normalized averaged minor radius, ρ. Figure 1 shows the radial profiles of the ECE signal at the midplane with $\phi = 324°$ (horizontally elongated cross section) and ion temperature (T_i) measured with CXS at the midplane of the plasma with $\phi = 342$ (vertically elongated cross section) for the plasmas with and without an island. The radial profiles of electron temperature and density show flattening due to the $n/m = 1/1$ magnetic island near the plasma edge in the plasma with the magnetic island ($I_{n/m=1/1} = 1200$ A), in contrast to the plasma without a magnetic island (there is a natural $n/m = 1/1$ island in LHD; however, the natural island can be canceled by the appropriate external field with $I_{n/m=1/1} = 390$ A). As seen in the ECE signal, the electron temperature profile for the plasma with a magnetic island shows the flattening in the region where the O point of the magnetic island is located [13]. The ion temperature profiles also show the clear flattening inside the magnetic island with a width of 9.0 ± 1.3 cm (from $R = 4.0$ m to $R = 4.09$ m) as well as electron profiles.

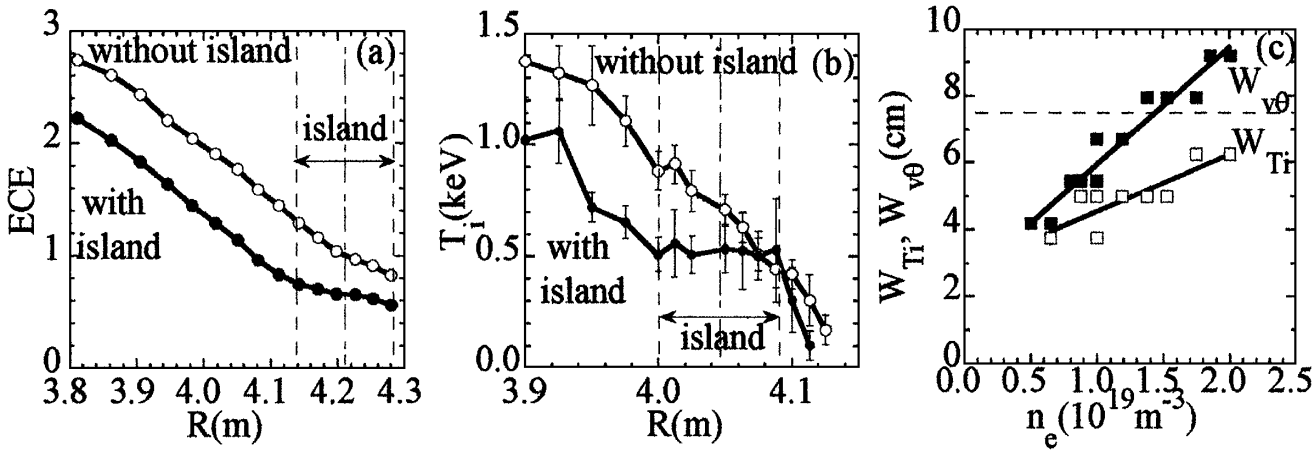

FIG. 1. Radial profiles of (a) ECE signal at a horizontally elongated cross section, and (b) ion temperature at a vertically elongated cross section with and without a magnetic island for the plasma with $B = 2.83$ T and $R_{ax} = 3.5$ m. (c) Density dependence of W_{Ti}, $W_{v\theta}$ measured for the plasma with $B = 1.5$ T and $R_{ax} = 3.5$ m. The dashed lines are island widths in the absence of plasma.

The density dependence of the widths of flattening of the ion temperature and the poloidal velocity profiles are studied for the plasma with fixed perturbation current, $I_{n/m=1/1} = 800$ A and with the magnetic field of 1.5 T. These widths are given by a least-squares fit (with constant weighting) of the measured profiles to the model profiles, where the ion temperature gradient is zero for $R_i - (1/2)W_{\mathrm{Ti}} < R < R_i + (1/2)W_{\mathrm{Ti}}$ and the poloidal velocity is zero for $R_i - (1/2)W_{v\theta} < R < R_i + (1/2)W_{v\theta}$. Here R_i is the major radius for the center of the magnetic island. The gradients are assumed to have constant, finite values up to 2.5 cm (three data points) outside the flattened region. In the least-squares fit to the model profiles, the smoothing due to the space resolution of the measurements is taken into account by convolving the model profiles with a Gaussian function of width 1.5 cm. As seen in Fig. 1(c), W_{Ti} shows weak dependence on the electron density. One of the important results from Fig. 1(c) is the fact that the $W_{v\theta}$ is always larger than the W_{Ti}. The W_{Ti} should be smaller than the actual width of the magnetic island, W_m, due to the perpendicular diffusion of heat inside the magnetic island. Since the poloidal flow just outside the magnetic island should be decelerated by trapped particles inside the magnetic island, $W_{v\theta}$ is expected to be larger than the actual width of the magnetic island, W_m. The difference between $W_{v\theta}$ and W_{Ti} ($W_{v\theta} > W_{\mathrm{Ti}}$) is considered to be due to the radial diffusion process.

When the current of the $n/m = 1/1$ external perturbation coils is small (see 260 A in Fig. 2), no flattening appears in the profile of the poloidal flow nor in the ion temperature. As the perturbation coil current increases, a clear structure associated with the magnetic island appears in the poloidal flow. As the perturbation coil current increases, the width of flattening of poloidal velocity also increases up to 9 cm, which corresponds to 17% of ρ. The toroidal rotation velocity is small, -0.7 ± 0.5 km/s for the plasma with island ($I_{n/m=1/1} = 900$ A) and -2.6 ± 0.6 km/s for the plasma without island ($I_{n/m=1/1} = 260$ A). Here negative values stand for the flow parallel to the $\langle E_r \times B_\theta \rangle$ direction of negative E_r. The contribution of toroidal flow and pressure gradient to E_r is negligibly small (<1 kV/m) and E_r and E_r shear are almost identical to $v_\theta \times B_\phi$ and $d(v_\theta \times B_\phi)/dr$.

In the model, E_r jumps at the boundary of the magnetic island, i.e., finite values outside the magnetic island and zero E_r inside the island. This is not correct because the boundary itself should have a finite width Δ due to the shear viscosity. This width is determined by the viscous coefficient μ and the ratio of radial electric field to radial current and is given by $\Delta = \sqrt{\mu \varepsilon_0 \varepsilon_\perp E_r / j_r}$, where $\varepsilon_0 \varepsilon_\perp$ is the dielectric constant and E_r, j_r are the radial electric field and neoclassical radial current needed to sustain the E_r outside the magnetic island, respectively [14]. The sheared width estimated by using this formula is consistent with the experimental value observed in the compact helical system (CHS) [15]. The value of shear width Δ is estimated to be 1.4 cm using the neoclassical current and radial electric field, $\varepsilon_0 \varepsilon_\perp E_r / j_r = 0.1$ ms and $\mu = 2$ m^2/s at $\rho = 0.9$. Here the radial current and radial electric field are estimated by neoclassical theory, while the perpendicular viscosity is assumed to be identical to the thermal diffusivity in LHD [16]. Although the shear width is much larger than the finite orbit width for neon ions (0.4 cm), it is not large enough to be measured with the CXS which has the spatial resolution of ± 1.5 cm. When the perturbation current, $I_{n/m=1/1}$, becomes large enough (see 1200 A in Fig. 2), the poloidal flow along the magnetic flux surface appears inside the magnetic island and the toroidal flow changes its sign (2.7 ± 1.2 km/s). The ion temperature profile clearly shows that the magnetic island is slightly expanded and does not shrink or disappear. It should be noted that the poloidal flow is zero at the center of the magnetic island

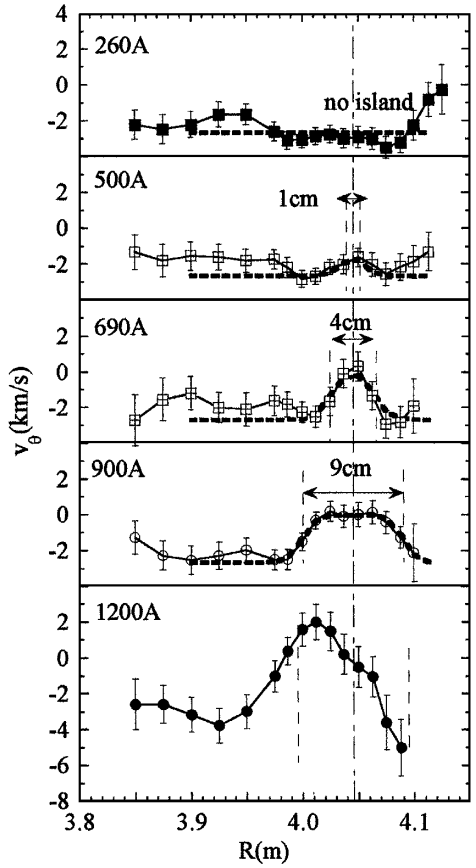

FIG. 2. Radial profiles of poloidal rotation velocity, for various currents of $n/m = 1/1$ external perturbation coils, in the plasma with $B = 1.5$ T and $R_{ax} = 3.5$ m. The last closed surfaces are at $R = 3.28$ m and $R = 4.10$ m at the cross section vertically elongated. The major radius for the center of island, R_i, is indicated with a line as a reference. The dashed lines are fitted profiles of poloidal velocity to the measured values.

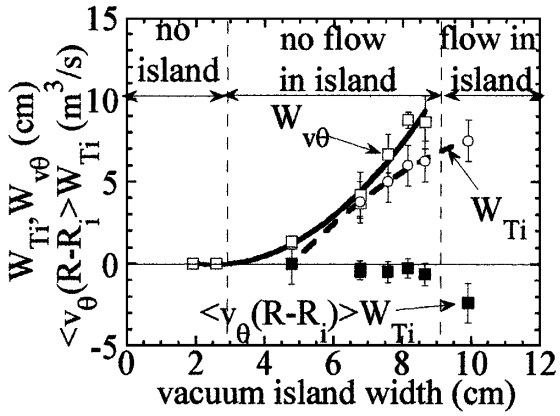

FIG. 3. The widths W_{Ti} and $W_{v\theta}$ estimated from the radial profiles of ion temperature and poloidal flow measured as a function of island width of the vacuum magnetic field W_{mvac} in the plasma with $B = 1.5$ T and $R_{ax} = 3.5$ m. The magnitude of flow inside the magnetic island, $\langle v_\theta(R - R_i)\rangle W_{\mathrm{Ti}}$, is also plotted.

and the direction of the flow is reversed across the center of the island.

As seen in Fig. 3, $W_{v\theta}$ and W_{Ti} are not proportional to the size of the magnetic island, W_{mvac}, calculated with external coil currents (island in vacuum). This is because there is a "self-healing" in the plasma, which suppresses the actual size of the magnetic island, W_m [13]. The transition to convective poloidal flow from zero poloidal flow inside the island is observed at a smaller sized vacuum magnetic island for the plasma with higher magnetic field or higher plasma density. As the indication of magnitude of convective flow, the quantity $\langle v_\theta(R - R_i)\rangle W_{\mathrm{Ti}}$, where $\langle \cdots \rangle$ stands for averaging along the midplane, is evaluated inside the flattened region of ion temperature profile as a measure which is proportional to the total angular momentum. This quantity is almost zero and slightly increases as the size of the magnetic island is increased. When the width of the vacuum magnetic island, W_{mvac}, exceeds 9 cm, then it sharply increases, which indicates the appearance of the flow along the magnetic flux surface inside the magnetic island. One of the candidates to explain this nonlinearity is the sudden loss of the reduction of flow viscosity due to the flow shear. The anomalous transport due to the turbulence is considered to decrease when the $\mathbf{E} \times \mathbf{B}$ shearing rate $\varpi_{\mathbf{E}\times\mathbf{B}}$ becomes large enough. An estimate of the threshold value of dE_r/dr in a heliotron configuration was given in [17], providing a value on the order of 1 MV m^{-2}. The lower limit of E_r shear and the shearing rate given by the measurements is 0.2–0.4 MV m^{-2} and 10^5 s^{-1} at the boundary of the magnetic island. The high flow shear observed suggests the reduction of the anomalous perpendicular viscosity of the plasma flow at the boundary of the magnetic island. The $\mathbf{E} \times \mathbf{B}$ turbulence suppression may play an important role to keep the sharp gradient of the poloidal flow in the regime with no flow inside the island. On the other hand, in the regime with flow inside the island, the $\mathbf{E} \times \mathbf{B}$ shearing rate drops below the critical value for turbulence suppression.

When the vacuum island width W_{mvac} is greater than the critical value discussed above, the poloidal flow along the magnetic flux surface appears inside the magnetic island, and the radial electric field no longer becomes constant inside the magnetic island. As seen in the radial profiles of the radial electric field in Fig. 4(a), the radial electric field is zero at the center of the magnetic island ($R = 4.045$ m) with the negative half of the magnetic island towards the plasma edge and the positive half of the magnetic island away from the plasma edge. Although the space potential inside the magnetic island is flat when the size of the vacuum island, W_{mvac}, is below the critical value, it has a positive/negative curvature ($d^2\Phi/dr^2 > 0$ or $d^2\Phi/dr^2 < 0$) depending on the sign of the velocity shear and the E_r shear at the x point of the magnetic island, when the vacuum island width, W_{mvac}, exceeds a critical value. As shown in Fig. 4(b), the curvature of the space potential

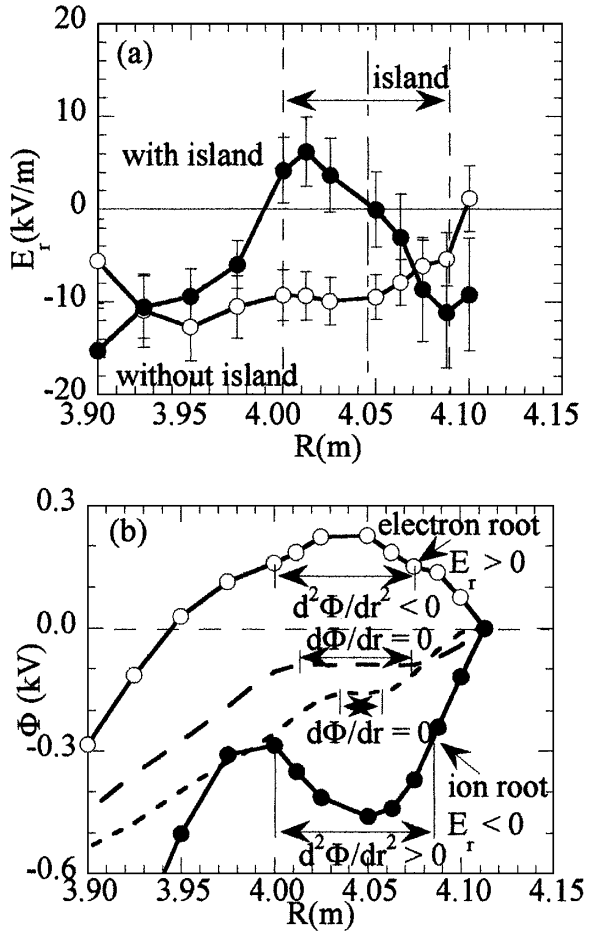

FIG. 4. Radial profiles of (a) radial electric field for the shots in Figs. 1(a) and 1(b), and (b) space potential given by integrating the radial electric field on the midplane for the plasmas with the flow (solid lines) inside the magnetic island in the ion root [$n_e = 1.7 \times 10^{19}$ m^{-3}, E_r (edge) < 0] and in the electron root [$n_e = 1.1 \times 10^{19}$ m^{-3}, E_r (edge) > 0]. The radial profiles of space potential without the flow (dashed lines) inside the magnetic island are also plotted as references.

$(d^2\Phi/dr^2)$ is positive in the ion root, where the E_r and E_r shear are negative, while it is negative in the electron root ($E_r > 0$ and $dE_r/dr > 0$) [18]. Since the flow along the magnetic flux surface inside the magnetic island is driven by the imbalance of viscous forces between the inside and outside of the magnetic island, its direction is considered to be determined by the sign of the velocity shear. It should be noted that the values of space potential at both sides of the boundary of the magnetic island are identical. These data demonstrate that the space potential is constant on the magnetic flux surface but not necessarily constant inside the magnetic island.

In conclusion the flattening of the ion temperature and space potential is observed inside the magnetic island when the $n/m = 1/1$ perturbation field is applied in LHD plasmas. The flattening of space potential is due to the damping of the poloidal flow inside the magnetic island. When the vacuum magnetic island width, W_{mvac}, exceeds the critical value (15%–20%) of minor radius, the flow along the magnetic flux surface inside the magnetic island in the direction to reduce the flow shear at the boundary of the magnetic island is observed. When a magnetic island rotates in the plasma frame ($\mathbf{E} \times \mathbf{B}$ rotating frame), there is no flow shear at the boundary of the magnetic island. In this experiment, the magnetic island itself does not rotate even with the existence of $\mathbf{E} \times \mathbf{B}$ rotation in the plasma, which causes the flow shear at the boundary of the magnetic island. Even in the rotating magnetic island, the flow shear at the boundary of the magnetic island can be important, when there is a difference in rotation velocity between the magnetic island and $\mathbf{E} \times \mathbf{B}$. The flow shear at the magnetic island is one of the candidates used to explain the correlation between the position of the transport barrier and the location of low order rational magnetic surface [19].

This work is partly supported by a grant-in-aid for scientific research of MEXT Japan. The authors thank Dr. A. Fujisawa and Dr. M. Tanaka for useful discussions and the technical support on LHD for the experiments. One of the authors (K. I.) acknowledges discussions with Professor S-I. Itoh and Dr. M. Yagi.

[1] P. C. de Vries *et al.,* Plasma Phys. Controlled Fusion **39**, 439 (1997).
[2] A. Weller *et al.,* Phys. Rev. Lett. **59**, 2303 (1987).
[3] R. D. Gill *et al.,* Nucl. Fusion **32**, 723 (1992).
[4] P. C. de Vries *et al.,* Nuclear Fusion **37**, 1641 (1997).
[5] H. Zohm *et al.,* Nucl. Fusion **13**, 197 (2001).
[6] H. Y. Kamada, Plasma Phys. Controlled Fusion **42**, A65 (2000).
[7] S-I. Itoh and K. Itoh, Comments Plasma Phys. Controlled Fusion **13**, 141 (1990).
[8] N. J. Lopes Cardozo *et al.,* Phys. Rev. Lett. **73**, 256 (1994).
[9] C. Hidalgo *et al.,* Plasma Phys. Controlled Fusion **42**, A153 (2000).
[10] M. Fujiwara *et al.,* Nucl. Fusion **40**, 1157 (2000).
[11] N. Ohyabu *et al.,* Phys. Rev. Lett. **84**, 103 (2000).
[12] K. Ida, S. Kado, and Y. Liang, Rev. Sci. Instrum. **71**, 2360 (2000).
[13] K. Narihara *et al.,* Phys. Rev. Lett. **87**, 135002 (2001).
[14] A. Fujisawa *et al.,* Phys. Rev. Lett. **82**, 2669 (1999).
[15] A. Fujisawa, Phys. Plasmas **7**, 4152 (2000).
[16] H. Yamada *et al.,* Phys. Rev. Lett. **84**, 1216 (2000).
[17] K. Itoh *et al.,* Plasma Phys. Controlled Fusion **36**, 123 (1994).
[18] K. Ida *et al.,* Phys. Rev. Lett. **86**, 5297 (2001).
[19] P. Mantica *et al.,* Phys. Rev. Lett. **82**, 5048 (1999).